Published online 28 June 2017

Nucleic Acids Research, 2017, Vol. 45, No. 15 ***e141***
doi: 10.1093/nar/gkx568

mRNA detection in budding yeast with single fluorophores

Gable M. Wadsworth[1,†], Rasesh Y. Parikh[1,†], John S. Choy[2] and Harold D. Kim[1,*]

[1]School of Physics, Georgia Institute of Technology, 837 State Street, Atlanta, GA 30332-0430, USA and
[2]Department of Biology, The Catholic University of America, 620 Michigan Avenue NE, Washington, DC 20064, USA

Received March 03, 2017; Revised June 06, 2017; Editorial Decision June 19, 2017; Accepted June 21, 2017

ABSTRACT

Quantitative measurement of mRNA levels in single cells is necessary to understand phenotypic variability within an otherwise isogenic population of cells. Single-molecule mRNA Fluorescence In Situ Hybridization (FISH) has been established as the standard method for this purpose, but current protocols require a long region of mRNA to be targeted by multiple DNA probes. Here, we introduce a new single-probe FISH protocol termed sFISH for budding yeast, *Saccharomyces cerevisiae* using a single DNA probe labeled with a single fluorophore. In sFISH, we markedly improved probe specificity and signal-to-background ratio by using methanol fixation and inclined laser illumination. We show that sFISH reports mRNA changes that correspond to protein levels and gene copy number. Using this new FISH protocol, we can detect >50% of the total target mRNA. We also demonstrate the versatility of sFISH using FRET detection and mRNA isoform profiling as examples. Our FISH protocol with single-fluorophore sensitivity significantly reduces cost and time compared to the conventional FISH protocols and opens up new opportunities to investigate small changes in RNA at the single cell level.

INTRODUCTION

Genetically identical cells are known to display phenotypic heterogeneity (1). This is due in large part to variation in gene expression from cell to cell (2,3). Such single-cell variability can increase fitness of both unicellular and multicellular organisms against unpredictable changes in the environment (4) and may lead to other mechanisms of biological importance (5,6). Hence, quantification of gene expression at the single cell level has become an active area of technological development. Transcription, which takes place in bursts at one or a few copies of a gene, is a significant source of gene expression noise, and therefore, measuring mRNA levels in single cells is essential to investigate noise generation mechanisms.

There are two general methods to quantify mRNA levels in single cells. The first type, which includes quantitative PCR (qPCR) and RNA sequencing (RNA-seq), relies on an indirect readout of DNA that is generated from reverse transcribed mRNA extracted from lysed cells. The main advantage of these methods is the scalability. Combined with a microfluidic or a single-cell sorting platform, these methods allow the whole transcriptome analysis of a single cell (7). However, these methods require laborious sample preparation and high-cost instruments, and are error-prone for short, low copy number transcripts (8). Due to the high cost of resources, these methods are in general not appropriate for a focused analysis of individual transcripts. These techniques also do not preserve information on subcellular localization of transcripts with respect to other cellular compartments, which may be valuable to understand their role and function (9).

In contrast, mRNA detection by fluorescence in situ hybridization (FISH) relies on a direct readout emanating from fluorescently labeled DNA probes bound to target mRNA molecules inside the cell. This method involves only low-cost cell processing and routine fluorescence microscopy and can yield absolute numbers for targeted transcripts without separate calibration steps. Since its first demonstration in 1982 (10), mRNA FISH has undergone significant advancement, now capable of detecting single-nucleotide variants (11) and gene fusions (12,13), and can be used to determine RNA sequence (14).

Currently, there are two widely used mRNA FISH protocols. The first protocol developed by the Singer lab (15,16) uses ∼50 nucleotide (nt) long probes that are each labeled with multiple fluorescent dyes. Five different probes, when hybridized to a single mRNA, generate an intense spot under a fluorescence microscope. The second protocol was introduced by Raj *et al.* (17), and features relatively short (∼20 nt) probes that are singly labeled. To compensate for the smaller number of fluorophores per probe, 20–50 probes are used to detect a single mRNA. Both protocols require the

*To whom correspondence should be addressed. Tel: +1 404 8940080; Fax: +1 404 8941101; Email: harold.kim@physics.gatech.edu
†These authors contributed equally to this work as first authors.

target transcript to be quite long (>200 nt) for hybridization of multiple probes (18,19).

The need of multiple probes is 2-fold. First, multiple probes increase the intensity of FISH spots. If N different probes can all bind to the same mRNA with equal probability, p, the mean number of probes per mRNA is Np. Secondly, using multiple probes increases the detection rate of mRNA because the probability of all N probes failing to bind an mRNA molecule is $(1 - p)^N$. Therefore, in principle, one can decrease the false negatives (the number of undetected mRNA molecules) by increasing the number of probes.

However, the multiple probe requirement is not absolute. In many studies, single mRNA molecules were successfully probed with a smaller number of fluorophores: as few as four fluorophores for budding yeast (20) and a single fluorophore for *Escherichia coli* (21). Recently, single nucleotide variants were detected at the single fluorophore level in human cells, albeit with multiple fluorophores of a different color used as a guide (11). Therefore, although considered difficult (22), detecting mRNA with a single fluorophore is achievable.

In many cases, mRNA FISH can be used for relative quantification of a specific transcript under different conditions or transcriptional heterogeneity in an isogenic population of cells. For such applications, the use of multiple probes is not needed. Reducing the number of probes may compromise the signal, but most FISH studies employ an epi-fluorescence microscope, which is not optimal for single-fluorophore detection with cellular background. We were thus motivated to revisit the current FISH method originally developed for budding yeast and explore the possibility of using single probes to measure relative abundance of mRNAs.

Here, we present single-fluorophore, single-probe FISH (sFISH) for budding yeast. In our modified method, a 26-nt probe with a single Cy3 or Cy5 dye is sufficient to accurately detect single mRNA molecules in single yeast cells. We employ methanol fixation and highly inclined laser illumination to increase the signal to noise ratio needed to capture fluorescence from single probes. We varied the transcription rate of a fluorescent reporter gene by changing the promoter strength and found that our new method could detect a proportional change in the corresponding mRNAs. By using three independent methods, we estimate the detection efficiency of this protocol at ∼60%. We anticipate that this method will add a highly useful tool for measuring steady-state transcript statistics of budding yeast. Technical improvements introduced in this protocol can also be used to study short transcripts in budding yeast.

MATERIALS AND METHODS

Strain construction

We constructed multiple PHO5 promoter variants of budding yeast following the protocol used in our previous study (23). These variants share a high affinity Pho4 binding site in the exposed region between nucleosome -2 and nucleosome -3, thus belonging to a family of HX promoter variants (24). These variants differ in their DNA sequence in the nucleosome -2 region (Supplementary Figure S1 and Supplementary Table S1). The PHO5 open reading frame was then replaced with a yellow fluorescent protein (yEVenus) gene by homologous recombination. To achieve constitutive expression of yEVenus, the PHO5 promoter variants were mated with the pho80Δ strain (25). yEVenus levels of these promoter variants were quantified using the epi-fluorescence microscope (Supplementary Figure S1B). Yeast strains with different ploidies (2N, 3N, 4N) were from Dr David Pellman.

Sample preparation

Our procedure closely follows the protocols by Youk *et al.* (26) and Raj *et al.* (27) with some modifications. Yeast cells are grown overnight to a final OD_{600} of 0.5 in 50 ml of SD complete medium. Cells are fixed and then kept at 4°C. Fixation is performed either by treating the cells with 2% (v/v) formaldehyde or with methanol for 10 min. In the case of methanol, cells are spun down, and the pellet is resuspended in methanol. The cells are washed twice with Buffer B (1.2 M sorbitol, 0.1 M potassium phosphate) at 4°C after fixation. Cells are then resuspended in 1 ml of spheroplasting buffer (10 ml Buffer B, 100 μl 200 mM vanadyl ribonucleoside complex from New England Biolabs). 2 μl of zymolyase at 5 units/μl (Zymolyase-20T at 21 000 units/g from Seikagaku Business Corporation) are added into the mixture of cells, and then they are incubated at 30°C. The amount of digestion is determined by measuring OD_{600} of 1 ml of a suspension containing 100 μl of the cell sample until the OD_{600} has decreased by ∼30%, which is typically 15 min. Cell wall digestion can be verified by allowing 10 μl cells to settle to the surface of a multi-well plate and adding 100 μl DI water to the well. Within a few minutes the majority of the cells should be lysed when inspected under a microscope. If the cells do not lyse, then the procedure has not effectively removed the cell wall. Following this treatment the cells are washed twice in Buffer B at 4°C and stored in 70% ethanol for at least 1 h.

Hybridization is performed by washing the cells twice with 1 ml of wash buffer containing 10% formamide and 330 mM salt as SSC buffer. This step loosens the protein–RNA interactions to increase RNA accessibility for probe hybridization, and decreases nonspecific probe binding (28). Hybridization buffer is prepared in 10 ml volumes containing 1 ml 20X SSC (Ambion), 1 ml Formamide (Ambion), 100 μl 200 mM vanadyl ribonucleoside complex (New England Biolabs), 1 g dextran sulfate sodium salt (Sigma, D8906), 10 mg *E. coli* tRNA (Sigma, R1753), 40 μl of 5 mg/ml BSA (Ambion), and 8 ml deionized water. Cells are resuspended in hybridization buffer and the appropriate amount of probes is added to bring the working concentration to 65 nM and the final volume to 100 μl. Cells are then incubated at 30°C overnight. The following morning, cells are washed twice in wash buffer and left as a pellet. Slides are prepared by mixing 2 μl of concentrated cells with 2 μl of imaging buffer that has the same concentration of salt as the wash and hybridization buffers. 1.5–2 μl of cell suspension is placed between a microscope slide (1″ × 3″) and a coverslip (#1.5, 18 mm × 18 mm), and the chamber is gently pressed to form a monolayer of

cells. The edges of the chamber are sealed with fast curing epoxy. The height of the chamber is estimated to be about 3 μm. Cells slightly squeezed in the chamber remain confined during the observation period. The imaging buffer contains the PCA/PCD oxygen scavenging system (29) to extend the photobleaching lifetime of the fluorophores. The imaging buffer is composed of 10 mM Tris at pH 8, 5 μl 20X SSC, 2.5 mM protocatechuic acid (PCA), 10 nM protocatechuate-3,4-dioxygenase (PCD), and 1 mM Trolox (6-hydroxy-2,5,7,8-tetramethylchroman-2-carboxylic acid).

Microscope setup

Our custom setup was built around a commercial microscope (IX81, Olympus) equipped with motorized translation in *z*-direction and a motorized filter wheel. We used 514 nm line from an Argon laser to excite yEVenus, a 532-nm solid state laser (LCX-532L-100, Oxxius) to excite Cy3, and a 640 nm solid state laser (1185055, Coherent) to excite Cy5. All lasers were coupled to a fiber optic, and the laser output from the fiber optic was collimated and focused at the back focal plane of the objective (Olympus UPlanSApo 100×/1.4 Oil). We mounted the fiber coupling onto a translational stage to vary the incidence angle of the excitation beam (Supplementary Figure S2).

Imaging

The laser power was set to produce 25 mW of power at the back focal plane of the objective. Z-stack images were acquired using an EMCCD (iXon plus, Andor) at 512 × 512 resolution every 0.2 μm step over 10 μm distance. The exposure time for the Cy5 channel was set to 100 ms. Hardware control and image acquisition were performed using Micromanager (30).

Analysis

We used the MATLAB Image Processing Toolbox to batch process each three dimensional image through a series of automated steps(Supplementary Figure S3). Cell segmentation is accomplished by applying edge detection to DIC images of the cells. The detected edges are connected using [1 × 4] structural elements and binary morphological dilation and erosion operations. Cells are further selected based on the ellipticity and area of the detected regions.

Fluorescence intensities in cellular regions were background-corrected by subtracting the mean intensity taken from the cell boundary. Protein fluorescence was determined by taking the sum of the pixels inside the cell boundary and normalizing by the area. In FISH images, all maximum intensity pixels in the 3 × 3 × 3 neighborhood are selected as candidate spots. Spot intensity was calculated by taking the average of pixel values in a diffraction-limited ellipsoid and subtracting the background value evaluated from the pixels bounding the ellipsoid. The histogram of spot intensities was fit with a sum of three Gaussian distributions (Supplementary Figure S12). The first peak centered around zero arises mostly from noise. The second peak corresponds to spatially-resolved single transcripts. The third peak is likely due to multiple overlapping transcripts because this peak grows with gene expression level.

The important aspect of our spot identification algorithm is that spots are called using a locally determined threshold over a single cell. Due to nonuniform illumination, cells near the edge of the field of view are weakly excited, and the FISH spots are significantly dimmer than those near the center of the field of view. Therefore, applying cell-specific threshold can mitigate this problem, and reduce false negatives. To correct for the nonuniform illumination, we also adopted a post-acquisition algorithm called Corrected Intensity Distributions using Regularized Energy minimization (CIDRE) (31) prior to segmentation.

RESULTS

Observation of single fluorophores *in vivo*

While the current FISH approaches have been successfully applied to quantify mRNA level at the single cell level, they are not applicable to studies that investigate short RNA molecules or changes in short regions of RNA because of the multiple-probe requirement. To circumvent these limitations, we sought to develop a single-probe FISH technique for budding yeast. The three parameters we considered as we began our modified FISH method was the dye molecule, the fixative, and imaging technique. We chose Cy5 over Cy3 because yeast autofluorescence is lower in the red channel than the green (32). In addition, we tried two different fixatives that may differentially contribute to the signal-to-noise of Cy5 (33).

We first acquired fluorescence images of cells of a positive control strain under epi-illumination. We were able to observe isolated fluorescent spots, but the signal-to-background ratio was poor. Hence, we tried illuminating the cells using an inclined geometry (Figure 1B). Highly inclined illumination excites a thin slice inside the cell, which leads to higher excitation intensity and lower out-of-focal plane background compared to epi-illumination (34). Using this setup, we observed a significant enhancement in the signal-to-noise ratio (Figure 1C and D). The oxygen scavenging system was also critical for detection of the isolated fluorescent spots. Two observations indicate that most of these spots arise from a single Cy5 molecule. First, their fluorescence intensities are comparable to the fluorescence intensity of single Cy5 molecules nonspecifically bound to the surface. Second, upon continuous excitation, most spots disappear in single photobleaching steps, consistent with a single Cy5 molecule (Supplementary Figures S5).

Correlation between spot count and mRNA level

To test the linearity of our sFISH protocol, we performed FISH on four different strains (Figure 2A) that express yEVenus at four different levels (Supplementary Figure S1B). We did not use a promoter inducible by external factors as different induction conditions may differentially affect the hybridization efficiency.

We compared the measured spot counts with yEVenus levels (Figure 2B). The spot count ranged from 2 to 32. We observed a good correlation between spot count and protein level, which argues that fluorescent spots are generated from

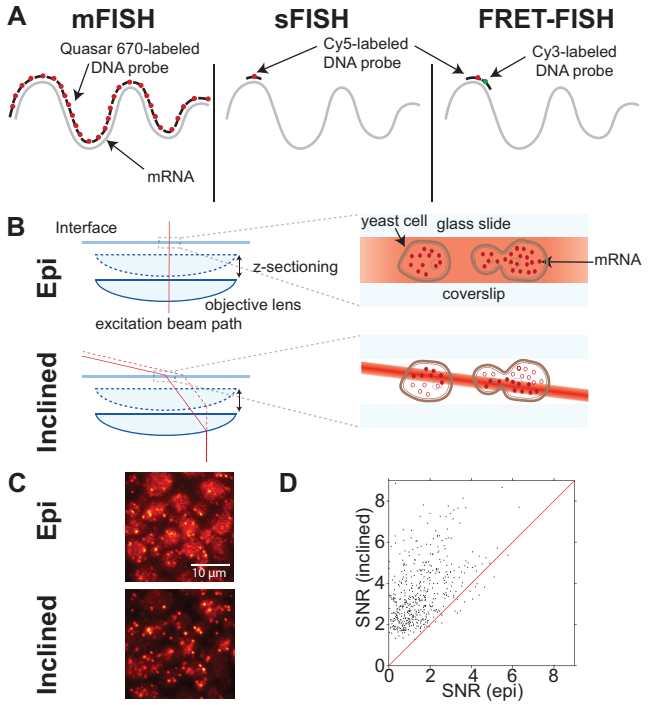

Figure 1. Comparison between single-probe FISH (sFISH) and multi-probe FISH (mFISH). yEVenus mRNA, which is 717-nt long, is probed by sFISH and mFISH. (**A**) Probe configurations are shown from left to right for 30 probe mFISH, sFISH and sFISH with FRET. For mFISH, we use a set of thirty Quasar 670 end-labeled probes. In sFISH, we use a single short Cy5-labeled DNA oligo probe. For FRET experiments the first Cy5-labeled probe is used in conjunction with a Cy3-labeled probe. (**B**) For mFISH, we use a conventional epi-fluorescence microscope setup (top). In epi-illumination, the beam is aligned along the optical axis and illuminates cells across their entire height. The difference in the beam intensity profile between the two geometries is highlighted by varying shades of red. For sFISH, we use highly inclined illumination geometry (bottom), which markedly increases the signal-to-noise ratio (SNR). This light sheet also travels with the objective, which allows imaging different planes along the vertical axis (z-sectioning). (**C**) The images shown are of the same field of view taken with epi-illumination (top) and then subsequently with inclined illumination (bottom) using the same laser power. The bottom image taken with inclined illumination exhibits more intense spots and lower background. (**D**) Comparison of spot signal-to-noise ratio (SNR) between epi- and inclined illumination. The SNR values measured with inclined illumination is plotted against those measured with epi-illumination. Most spots are found above the red line $y = x$, which indicates inclined illumination produces higher SNR than epi-illumination. The increase in signal to noise ratio is a factor of 2.15 on average.

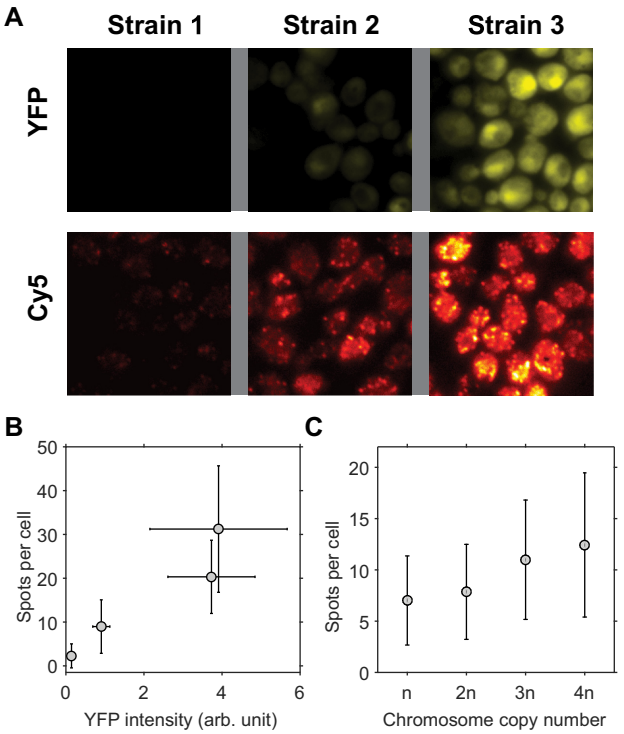

Figure 2. Correlation between sFISH spots and protein expression level. (**A**) Fluorescence images of single yeast cells expressing YFP (top row) and sFISH signals from Cy5-labeled probes targeting YFP mRNA (bottom row). Shown from left to right are fluorescence images of the negative control (no YFP expression), low YFP expression, and high YFP expression. Fluorescence intensities in the YFP channel and Cy5 channel are represented by false yellow and red colors, respectively. YFP images are from formaldehyde fixed cells, and Cy5 sFISH images are from methanol fixed cells. (**B**) Correlation plot. The mean number of FISH spots is plotted versus the mean yEVenus expression level. The error bars are measures of the standard deviation. (**C**) sFISH spots versus ploidy. sFISH was performed on yeast strains with four different ploidies (1n, 2n, 3n, 4n). The error bars show the standard deviation of the data. The number of spots detected per cell increases monotonically with the number of copies.

specific hybridization of the probe to the target mRNA. It also indicates that our spot counting algorithm works well in the range of transcript levels tested.

As another control, we performed sFISH on chromosome copy number variants (1n, 2n, 3n and 4n). We chose to probe a constitutively expressed gene KAP104 (Supplementary Tables S4 and S5), which has been used as a reference gene in other studies (35,36). As expected, the number of spots monotonically increased with the ploidy (Figure 2C), but interestingly, the relationship was not linear, that is, doubling the ploidy did not lead to doubling of the number of spots. This apparent sub-linear relationship could be due to the loss of extra chromosomes or some compensation effect, which will be the subject of future investigation.

In other controls, we were able to mask these sFISH spots with an unlabeled competitor probe in a concentration dependent manner (Supplementary Figure S4C and D), which confirms that the observed sFISH spots are due to the fluorescent probe hybridized to the KAP104 transcript. We also compared sFISH with mFISH (Supplementary Figure S4A). mFISH yielded an average of 9.4 spots per cell, similar to the number previously reported (35,36). In comparison, sFISH yielded less spots per cell than mFISH (6.5, Supplementary Figure S4B), which suggests that sFISH can detect the KAP104 transcripts with detection efficiency (p) of about 64% taking into account the false positive rate (0.5 spots per cell, Supplementary Figure S4D).

Methanol versus formaldehyde

We initially tried methanol as a fixative following a fast FISH protocol (37), and noticed that fluorescence images looked more clear than when using formaldehyde as the fixative. Hence, we performed a systematic comparison of the two fixatives. We first compared the number of background

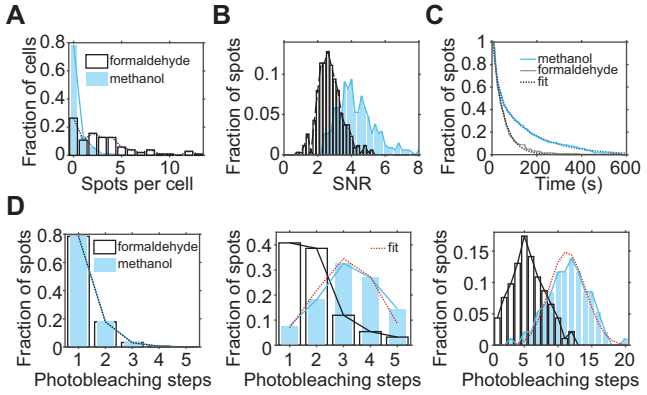

Figure 3. Comparison of spot quality between formaldehyde (white) treated samples and methanol (blue) treated samples. (**A**) sFISH spots detected from the negative control strain. On average, there is ∼0.3 spots per cell in the methanol treated cells (blue) compared to ∼3.1 spots per cell in the formaldehyde treated sample (white). (**B**) Comparison of signal-to-noise ratio (SNR) of single probes. SNR of a single Cy5 was calculated from fluorescence time traces that captured single-step photobleaching events. Signal is obtained from the single-step drop in fluorescence intensity upon photobleaching, and the noise is calculated as the standard deviation of the signal prior to photobleaching. The histogram shows that the spots from methanol-treated cells (blue) have ∼2-fold higher SNR than those from formaldehyde-treated cells (white). (**C**) Comparison of Cy5 stability. The population decay curves show that sFISH spots in formaldehyde treated cells photobleach faster than those in methanol-treated cells. (**D**) Comparison of probe number per spot. The number of probes per spot was determined by counting the number of photobleaching steps in the fluorescence time trace. When a single probe was used, most spots photobleached in a single step regardless of the fixative of choice (left). In comparison, when five (middle) or 30 (right) probes targeting the same mRNA were used, more probes were detected from spots in methanol-treated cells than in formaldehyde-treated cells. For the methanol samples treated with multiple probes (middle and right panels), binomial distribution fits are shown in red. For the five-probe experiment (5-probe FISH), Cy5-labeled probes and inclined illumination are used; whereas, for the thirty-probe experiment, Quasar-labeled dyes and epi-illumination are used.

spots in a negative control strain lacking the yEVenus gene between the two fixatives (Supplementary Figure S8). We found on average 3 spots per cell in formaldehyde-fixed cells compared to 0.3 spots per cell in methanol fixed cells, which indicate that formaldehyde fixation causes more nonspecifically bound or trapped Cy5 probes inside the cell (Figure 3A). Next, we compared the number of spots in a positive control strain with the lowest expression level of yEVenus. In this strain, we detected on average 10 spots per cell with methanol and three spots per cell with formaldehyde (Supplementary Figure S7). This result suggests that methanol fixation not only reduces nonspecific binding but also increases the rate of specific binding to the target mRNA.

With methanol-fixed cells, we not only detected more spots per cell in the positive control strain, but also detected more fluorophores per spot when multiple probes were used. To count the number of fluorophores per spot, we acquired time series of fluorescence from single spots in a fixed plane until they were completely photobleached. The histograms of the number of photobleaching steps are shown (Figure 3D). When a single probe was used, most spots photobleached in a single step in both methanol and formaldehyde-fixed cells. Spots that photobleached in two steps are likely due to close proximity of different mRNA molecules. As the number of probes was increased (1, 5 and 30), the difference in the number of photobleaching steps between formaldehyde and methanol treated samples became more noticeable. This measurement confirms that methanol fixation allows more efficient hybridization of probes to mRNA while preserving an improved signal-to-noise ratio.

This data also allows us to estimate the hybridization efficiency of probes. Assuming that probes all hybridize with the same probability p, the number of probes per spot can be fitted with a binomial distribution. We fitted the binomial distribution to the two sets of data taken with methanol fixation (red dotted lines, Figure 3D). p for yEVenus is extracted to be 61% for 5-probe FISH, and 38% for the 30-probe mFISH (Supplementary Table S3). The variation in p between the two data could be due to the difference in probe design. In 5-probe FISH, the probes were designed to have similar melting temperatures to the probe used for sFISH (shown in Supplementary Table S2), while in mFISH, the probes are designed to have the same length with no consideration of the melting temperature. Also, poor signal of Quasar 670 used in mFISH can lead to the underestimation of the number of photobleaching steps. Nonetheless, these rough estimates set the detection efficiency in the range of ∼40% to 60%.

We also characterized some apparent differences in the fluorescence properties of Cy5 due to the difference in fixatives. The fluorescence signal, which is defined as the difference between the fluorescence and background levels, was similar between the two. However, the noise, which is the fluctuation of the Cy5 signal, was significantly higher in formaldehyde fixed cells. As a result, the signal-to-noise ratio was 2-fold higher in methanol-fixed cells (Figure 3B). In addition to having an advantage in signal to noise ratio, methanol treated cells exhibited a longer Cy5 lifetime (Figure 3C).

Detection efficiency

To ensure that our FISH protocol operates at maximum hybridization efficiency, we increased zymolyase incubation time or the probe concentration until the spot count did not increase further (Supplementary Figures S9–S11). Even under this condition, however, our single-probe protocol is expected to underestimate the actual number of mRNA transcripts due to hindered accessibility of the target region of some transcripts. We can also estimate the effective detection efficiency (p) for the yEVenus transcript by increasing the number of probes. The number of spots detected per cell initially increased with the number of probes, but soon plateaued at four to five probes (Supplementary Figure S6). Assuming that each probe binds the target mRNA with probability p, the probability of failing to detect an mRNA molecule with n probes is $(1-p)^n$. Therefore, the number of detected spots (y) should increase with the number of probes (x) as $y \propto 1-(1-p)^x$. We fitted this model to the plot of the spot count per cell vs. probe number (Figure 4) and extracted p for the yEVenus transcript to be 53%, which is consistent with the range determined in the previous analysis (Figure 3).

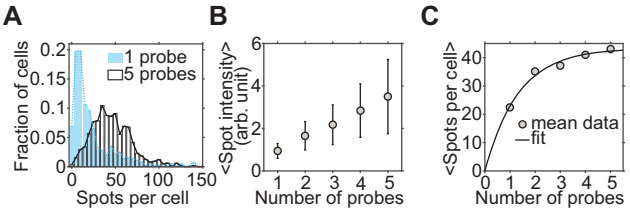

Figure 4. Estimation of the hybridization efficiency of single probes. (**A**) The effect of varying the number of probes. The histograms of the number of spots detected per cell are plotted for 1-probe (blue) and 5-probe (white) FISH. (**B**) Spot intensity vs. probe number. The mean spot intensity increases linearly with the number of probes as expected from the binomial distribution. (**C**) Spot number versus probe number. The mean number of spots detected per cell (y) increases with the number of probes (x). The fit model is $y = N(1 - (1 - p)^x)$ where N is the true copy number, and p is the hybridization rate for a single probe. p is extracted to be 53%.

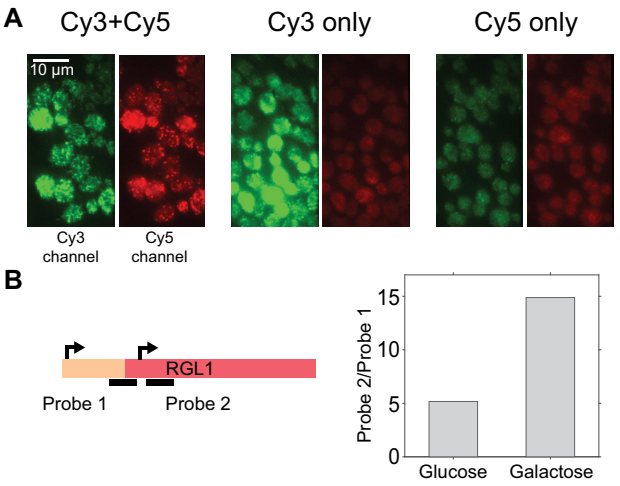

Figure 5. Applications of sFISH. (**A**) Demonstration of FRET-FISH in yeast. Fluorescence image acquired under 532-nm excitation was split into two half images based on the emission wavelength. In each image, the green half on the left is from the Cy3 emission channel, and the red half on the right is from the Cy5 emission channel. The images shown represent cells treated with both Cy3- and Cy5-probes (left), Cy3-probe only (middle), and Cy5-probe only (right). Bright, punctate spots were observed in the Cy5 channel only when cells were treated with both probes (left). (**B**) sFISH for mRNA isoform detection. The schematic on the left depicts alternative transcription initiation sites (arrows) at the RGL1 locus, which lead to mRNA isoforms with different lengths. Transcription from the first site produces a full-length mRNA, while from the second site produces a truncated isoform. Using sFISH with two separate probes, the relative fractions of these isoforms can be measured. Probe 1 targets the longer isoform only, whereas probe 2 targets both. The bar plot on the right shows the ratio of sFISH signals with probe 2 to probe 1 measured with glucose (left) or galactose (right) growth media. Here, the mean total fluorescence intensity per cell was used as a proxy for sFISH signal because transcription level was too high to count individual spots.

mRNA detection via FRET

In addition to various methods used above to infer the detection efficiency p, we also tried to determine p using Förster Resonance Energy Transfer (FRET). In this approach, two DNA probes complementary to immediately adjacent regions of the mRNA are labeled with donor (Cy3) and acceptor (Cy5), respectively, so that the FRET signal would arise only when both probes bind to the same mRNA (Figure 1A). By comparing the number of fluorescent spots due to FRET to the number of fluorescent spots due to direct excitation, the detection efficiency can be directly determined.

sFISH was performed with donor and acceptor probes at 1:1 ratio at the same concentration used for other experiments. As controls, sFISH was also performed while leaving out one of the probes. The typical sFISH images from three different combination of probes are presented in Figure 5. Upon 532 nm excitation, signal in the Cy5 channel was visible only when Cy3 probe is present (left, Figure 5), which indicates that many mRNA molecules are hybridized with both the Cy3-probe and Cy5-probe. We confirmed that this intense Cy5 signal could not have resulted from bleedthrough of Cy3 signal into the Cy5 channel (middle, Figure 5) or direct excitation of Cy5 by the 532nm laser (right, Figure 5). Upon 532-nm excitation, spots that appear in the Cy5 channel are due to FRET from the Cy3-probe to the Cy5-probe bound to the same mRNA. On the other hand, spots in the Cy3 channel arise from mRNA molecules bound with the Cy3-probe only. We can thus estimate the detection efficiency by dividing the number of Cy5 spots by the total number of both Cy3 and Cy5 spots. Using this method, the detection efficiency is determined to be 48%.

mRNA isoform detection via sFISH

Since sFISH requires only a 20–30 nt RNA target, it can be used to differentiate mRNA isoforms that are only slightly different in length or sequence, thus offering more versatility than mFISH. As a proof of principle, we chose gene RGL1 (YPL066W), which exhibits differential usage of alternative transcription sites between glucose and galactose growth media (38) (Supplementary Figure S13). As shown in the simplified schematic in Figure 5B, initiation normally starts upstream of the open reading frame (ORF) of RGL1 and produces a full-length transcript, but it can also start within the ORF and produce a truncated isoform. To measure the isoform profile, we designed a pair of probes (Supplementary Figure S13, Supplementary Table S6) that flank the truncation site (solid lines, Figure 5B) and performed sFISH with each probe on yeast cells grown in glucose and galactose media. Since the transcription levels were too high for reliable spot counting, we instead used the total fluorescence intensity integrated over the volume of the cell as a proxy for the transcription level. In qualitative agreement with the genome-wide transcript isoform study (38), we found that the truncated isoform is significantly enriched over the full-length isoform in galactose-containing media (Figure 5B).

DISCUSSION

In this work, we show that mRNAs in single yeast cells can be quantified using only a single ∼20-nt probe labeled with a single Cy5 dye. In this new yeast FISH protocol, we substantially improved signal-to-noise ratio and detection efficiency compared to current protocols by using a combination of methanol fixation and inclined illumination. We measured the detection efficiency *in situ* based on (i) the number of spots obtained with sFISH and mFISH, (ii) the

number of photobleaching steps per fluorescent spot, (iii) the number of fluorescent spots per cell, and (iv) the number of fluorescent spots due to FRET. These methods yielded detection efficiencies above 50% with some variability possibly due to the difference in probe sequence and length.

To detect single Cy5-labeled probes in situ, we used a lab-built fluorescence microscope with single molecule sensitivity. In this setup, 640-nm laser is focused off-center at the back focal plane of a high NA objective to obtain highly inclined illumination. Inclined illumination excites a smaller volume compared to epi-illumination, leading to a higher signal and lower background. We expect more advanced light-sheet microscopy setups (39–42) to perform equally well or better but they would require a specialized sample chamber for side-illumination. In principle, imaging flow cytometers with an extended depth of field can be used to increase throughput for counting fluorescent spots (43). Whether their sensitivity is sufficient to measure sFISH spots needs to be tested in the future.

We used backbone-integrated Cy5, which has a higher photostability (14) than base-linked Cy5 used in previous studies. Photobleaching lifetime of Cy5 is extended into minutes using PCA-based oxygen scavenging (29). Since the PCA-based system does not have heme groups or flavins, it also exhibits lower autofluorescence than glucose-based oxygen scavenging system.

Methanol, which is the fixative used in sFISH, perforates the cell membrane (44) by removing the phospolipids (45). Hence, the methanol-based method requires less stringent zymolyase treatment for probe delivery compared to formaldehyde-based method. The optimal digestion condition is important for accurate quantification of mRNA level; underdigestion leads to false negatives whereas overdigestion leads to leakage of cytoplasmic material including mRNA. However, we find it difficult to generate a uniformly digested population of cells using zymolyase only. In comparison, the combination of methanol treatment with mild zymolyase treatment produces uniformly permeable population of cells in a reproducible manner.

In contrast to the cross-linking agent formaldehyde, methanol also induces denaturation of cellular proteins (46) including mRNA binding proteins (47), which may explain the increase in hybridization efficiency (48) and reduction of cellular autofluorescence (49,50). In comparison, formaldehyde is known to modify the amine group available in nucleic acids (51), most notably in the guanine base (52), which will inevitably compromise hybridization efficiency. Moreover, we observed that formaldehyde fixation gave rise to higher background.

Our sFISH method can detect up to 64% of mRNA transcripts (See Supplementary Figure S4D), which is similar to the detection efficiencies reported in other FISH studies (61% in budding yeast (20,53), ∼65% (11) in human melanoma cells, and 70% (54) in CHO cells). The detection efficiency extracted from our in situ analysis is also consistent with the fact that our sFISH yields about half as many spots as mFISH does for both the PHO5 mutant (24,55,56) and KAP104 (36).

Spot counting becomes difficult when the transcript level is high because spots begin to overlap with one another. In such cases, the total fluorescence intensity from a single cell can be used to extrapolate the transcript level (55,57,58). Compared to mFISH, our sFISH produces spots with more uniform intensities because mRNA is associated with a single fluorophore, and therefore, the total fluorescence intensity would be a robust proxy for the transcript level.

Our sFISH method not only offers a time- and cost-efficient mRNA quantification tool, but also opens up new opportunities for transcript research at the single cell level. Owing to its much smaller target size compared to mFISH, sFISH can be used to detect RNA shorter than 100 nt, profile mRNA isoforms (38,59,60), detect subtle changes in mRNA sequence over a 30-nt window as a result of alternative splicing (61–63) and to measure transcriptional (64) and degradational intermediates (65) with improved resolution. FRET-FISH, which we demonstrated here, can also be used to detect circular RNA (66) in situ without an amplification step.

CONCLUSION

We demonstrate sFISH to be possible and viable for budding yeast cells. Through the combination of highly inclined illumination and methanol fixation, improved accuracy and consistency in quantification of mRNA level can be achieved. This method also yields comparable results to mFISH protocol at a reduced cost. We envision this method to be particularly useful for quantification of a short stretch of RNA at the single cell level.

SUPPLEMENTARY DATA

Supplementary Data are available at NAR Online.

ACKNOWLEDGEMENTS

This work is supported by Georgia Institute of Technology startup funds, GAANN Molecular Biophysics and Biotechnology Fellowship, and the National Institutes of Health grant (R01-GM112882). J.S.C. thanks the Litovitz Family Fund for support.

FUNDING

National Institutes of Health [R01-GM112882]. Funding for open access charge: National Institutes of Health [R01-GM112882].
Conflict of interest statement. None declared.

REFERENCES

1. Sumner,E.R. and Avery,S.V. (2002) Phenotypic heterogeneity: differential stress resistance among individual cells of the yeast Saccharomyces cerevisiae. *Microbiology*, **148**, 345–351.
2. Elowitz,M.B., Levine,A.J., Siggia,E.D. and Swain,P.S. (2002) Stochastic gene expression in a single cell. *Science*, **297**, 1183–1186.
3. Raser,J.M. and O'shea,E.K. (2005) Noise in gene expression: origins, consequences, and control. *Science*, **309**, 2010–2013.
4. Ackermann,M. (2015) A functional perspective on phenotypic heterogeneity in microorganisms. *Nat. Rev. Microbiol.*, **13**, 497–508.
5. Symmons,O. and Raj,A. (2016) What's luck got to do with it: single cells, multiple fates, and biological nondeterminism. *Mol. Cell*, **62**, 788–802.

6. Hewitt,S.K., Foster,D.S., Dyer,P.S. and Avery,S.V. (2016) Phenotypic heterogeneity in fungi: importance and methodology. *Fungal Biol. Rev.*, **30**, 176–184.
7. Kolodziejczyk,A.A., Kim,J.K., Svensson,V., Marioni,J.C. and Teichmann,S.A. (2015) The technology and biology of single-cell RNA sequencing. *Mol. Cell*, **58**, 610–620.
8. Saliba,A.-E., Westermann,A.J., Gorski,S.A. and Vogel,J. (2014) Single-cell RNA-seq: advances and future challenges. *Nucleic Acids Res.*, **42**, 8845–8860.
9. Crosetto,N., Bienko,M. and van Oudenaarden,A. (2015) Spatially resolved transcriptomics and beyond. *Nat. Rev. Genet.*, **16**, 57–66.
10. Singer,R.H. and Ward,D.C. (1982) Actin gene expression visualized in chicken muscle tissue culture by using in situ hybridization with a biotinated nucleotide analog. *Proc. Natl. Acad. Sci. U.S.A.*, **79**, 7331–7335.
11. Levesque,M.J., Ginart,P., Wei,Y. and Raj,A. (2013) Visualizing SNVs to quantify allele-specific expression in single cells. *Nat. Methods*, **10**, 865–867.
12. Markey,F.B., Ruezinsky,W., Tyagi,S. and Batish,M. (2014) Fusion FISH imaging: single-molecule detection of gene fusion transcripts in situ. *PLoS One*, **9**, e93488.
13. Semrau,S., Crosetto,N., Bienko,M., Boni,M., Bernasconi,P., Chiarle,R. and van Oudenaarden,A. (2014) FuseFISH: robust detection of transcribed gene fusions in single cells. *Cell Rep.*, **6**, 18–23.
14. Lee,J.H., Daugharthy,E.R., Scheiman,J., Kalhor,R., Yang,J.L., Ferrante,T.C., Terry,R., Jeanty,S.S., Li,C., Amamoto,R. *et al.* (2014) Highly multiplexed subcellular RNA sequencing in situ. *Science*, **343**, 1360–1363.
15. Long,R., Elliott,D.J., Stutz,F., Rosbash,M. and Singer,R.H. (1995) Spatial consequences of defective processing of specific yeast mRNAs revealed by fluorescent in situ hybridization. *RNA*, **1**, 1071.
16. Levsky,J.M. and Singer,R.H. (2003) Fluorescence in situ hybridization: past, present and future. *J. Cell Sci.*, **116**, 2833–2838.
17. Raj,A., Van Den Bogaard,P., Rifkin,S.A., Van Oudenaarden,A. and Tyagi,S. (2008) Imaging individual mRNA molecules using multiple singly labeled probes. *Nat. Methods*, **5**, 877.
18. Perriman,R.J. and Ares,M. Jr (2011) Alternative splicing variability: exactly how similar are two identical cells? *Mol. Syst. Biol.*, **7**, 505.
19. Gaspar,I. and Ephrussi,A. (2015) Strength in numbers: quantitative single-molecule RNA detection assays. *Wiley Interdiscipl. Rev.: Dev. Biol.*, **4**, 135–150.
20. Lubeck,E. and Cai,L. (2012) Single-cell systems biology by super-resolution imaging and combinatorial labeling. *Nat. Methods*, **9**, 743–748.
21. Taniguchi,Y., Choi,P.J., Li,G.-W., Chen,H., Babu,M., Hearn,J., Emili,A. and Xie,X.S. (2010) Quantifying E. coli proteome and transcriptome with single-molecule sensitivity in single cells. *Science*, **329**, 533–538.
22. Itzkovitz,S. and van Oudenaarden,A. (2011) Validating transcripts with probes and imaging technology. *Nat. Methods*, **8**, S12–S19.
23. Parikh,R.Y. and Kim,H.D. (2013) The effect of an intervening promoter nucleosome on gene expression. *PLoS One*, **8**, e63072.
24. Kim,H.D. and O'Shea,E.K. (2008) A quantitative model of transcription factor–activated gene expression. *Nat. Struct. Mol. Biol.*, **15**, 1192–1198.
25. Kaffman,A., Herskowitz,I., Tjian,R. and O'Shea,E.K. (1994) Phosphorylation of the transcription factor PHO4 by a cyclin-CDK complex, PHO80-PHO85. *Science*, **263**, 1153–1156.
26. Youk,H., Raj,A. and van Oudenaarden,A. (2010) Imaging single mRNA molecules in yeast. *Methods Enzymol.*, **470**, 429–446.
27. Raj,A. and Tyagi,S. (2010) Detection of individual endogenous RNA transcripts *in situ* using multiple singly labeled probes. *Methods Enzymol.*, **472**, 365–386.
28. Trcek,T., Chao,J.A., Larson,D.R., Park,H.Y., Zenklusen,D., Shenoy,S.M. and Singer,R.H. (2012) Single-mRNA counting using fluorescent in situ hybridization in budding yeast. *Nat. Protoc.*, **7**, 408–419.
29. Aitken,C.E., Marshall,R.A. and Puglisi,J.D. (2008) An oxygen scavenging system for improvement of dye stability in single-molecule fluorescence experiments. *Biophys. J.*, **94**, 1826–1835.
30. Edelstein,A.D., Tsuchida,M.A., Amodaj,N., Pinkard,H., Vale,R.D. and Stuurman,N. (2014) Advanced methods of microscope control using μManager software. *J. Biol. Methods*, **1**, e10.
31. Smith,K., Li,Y., Piccinini,F., Csucs,G., Balazs,C., Bevilacqua,A. and Horvath,P. (2015) CIDRE: an illumination-correction method for optical microscopy. *Nat. Methods*, **12**, 404–406.
32. Sheff,M.A. and Thorn,K.S. (2004) Optimized cassettes for fluorescent protein tagging in Saccharomyces cerevisiae. *Yeast*, **21**, 661–670.
33. Spear,R.N., Li,S., Nordheim,E.V. and Andrews,J.H. (1999) Quantitative imaging and statistical analysis of fluorescence in situ hybridization (FISH) ofAureobasidium pullulans. *J. Microbiol. Methods*, **35**, 101–110.
34. Tokunaga,M., Imamoto,N. and Sakata-Sogawa,K. (2008) Highly inclined thin illumination enables clear single-molecule imaging in cells. *Nat. Methods*, **5**, 159–161.
35. Zenklusen,D., Larson,D.R. and Singer,R.H. (2008) Single-RNA counting reveals alternative modes of gene expression in yeast. *Nat. Struct. Mol. Biol.*, **15**, 1263–1271.
36. Dodson,A.E. and Rine,J. (2015) Heritable capture of heterochromatin dynamics in Saccharomyces cerevisiae. *Elife*, **4**, e05007.
37. Shaffer,S.M., Wu,M.-T., Levesque,M.J. and Raj,A. (2013) Turbo FISH: a method for rapid single molecule RNA FISH. *PLoS One*, **8**, e75120.
38. Pelechano,V., Wei,W. and Steinmetz,L.M. (2013) Extensive transcriptional heterogeneity revealed by isoform profiling. *Nature*, **497**, 127.
39. Huisken,J. and Stainier,D.Y. (2009) Selective plane illumination microscopy techniques in developmental biology. *Development*, **136**, 1963–1975.
40. Weber,M. and Huisken,J. (2011) Light sheet microscopy for real-time developmental biology. *Curr. Opin. Genet. Dev.*, **21**, 566–572.
41. Gao,L., Shao,L., Chen,B.-C. and Betzig,E. (2014) 3D live fluorescence imaging of cellular dynamics using Bessel beam plane illumination microscopy. *Nat. Protoc.*, **9**, 1083–1101.
42. Galland,R., Grenci,G., Aravind,A., Viasnoff,V., Studer,V. and Sibarita,J.-B. (2015) 3D high-and super-resolution imaging using single-objective SPIM. *Nat. Methods*, **12**, 641–644.
43. Maguire,O., Wallace,P.K. and Minderman,H. (2016) Fluorescent in situ hybridization in suspension by imaging flow cytometry. *Imaging Flow Cytometry: Methods Protoc.*, **1389**, 111–126.
44. Kalejta,R.F., Shenk,T. and Beavis,A.J. (1997) Use of a membrane-localized green fluorescent protein allows simultaneous identification of transfected cells and cell cycle analysis by flow cytometry. *Cytometry*, **29**, 286–291.
45. DiDonato,D. and Brasaemle,D.L. (2003) Fixation methods for the study of lipid droplets by immunofluorescence microscopy. *J. Histochem. Cytochem.*, **51**, 773–780.
46. Herskovits,T.T., Gadegbeku,B. and Jaillet,H. (1970) On the structural stability and solvent denaturation of proteins I. Denaturation by the alcohols and glycols. *J. Biol. Chem.*, **245**, 2588–2598.
47. Heym,R.G. and Niessing,D. (2012) Principles of mRNA transport in yeast. *Cell. Mol. Life Sci.*, **69**, 1843–1853.
48. Raška,I. (2003) Oldies but goldies: searching for Christmas trees within the nucleolar architecture. *Trends Cell Biol.*, **13**, 517–525.
49. Guillot,P.V., Xie,S.Q., Hollinshead,M. and Pombo,A. (2004) Fixation-induced redistribution of hyperphosphorylated RNA polymerase II in the nucleus of human cells. *Exp. Cell Res.*, **295**, 460–468.
50. Moter,A. and Göbel,U.B. (2000) Fluorescence in situ hybridization (FISH) for direct visualization of microorganisms. *J. Microbiol. Methods*, **41**, 85–112.
51. Millar III,D.B., Cukier,R. and Nirenberg,M. (1965) Interaction of Escherichia coli ribosomal ribonucleic acid with synthetic polynucleotides. Sedimentation properties, and thermal stability as measured by fluroescence polarization. *Biochemistry*, **4**, 976–985.
52. Lu,K., Ye,W., Zhou,L., Collins,L.B., Chen,X., Gold,A., Ball,L.M. and Swenberg,J.A. (2010) Structural characterization of formaldehyde-induced cross-links between amino acids and deoxynucleosides and their oligomers. *J. Am. Chem. Soc.*, **132**, 3388–3399.
53. Lubeck,E., Coskun,A.F., Zhiyentayev,T., Ahmad,M. and Cai,L. (2014) Single-cell in situ RNA profiling by sequential hybridization. *Nat. Methods*, **11**, 360–361.
54. Jungmann,R., Avendaño,M.S., Dai,M., Woehrstein,J.B., Agasti,S.S., Feiger,Z., Rodal,A. and Yin,P. (2016) Quantitative super-resolution imaging with qPAINT. *Nat. Methods*, **13**, 439–442.

55. Mao,C., Brown,C.R., Falkovskaia,E., Dong,S., Hrabeta-Robinson,E., Wenger,L. and Boeger,H. (2010) Quantitative analysis of the transcription control mechanism. *Mol. Syst. Biol.*, **6**, 431.
56. Brown,C.R., Mao,C., Falkovskaia,E., Jurica,M.S. and Boeger,H. (2013) Linking stochastic fluctuations in chromatin structure and gene expression. *PLoS Biol.*, **11**, e1001621.
57. Skinner,S.O., Sepúlveda,L.A., Xu,H. and Golding,I. (2013) Measuring mRNA copy number in individual Escherichia coli cells using single-molecule fluorescent in situ hybridization. *Nat. Protoc.*, **8**, 1100–1113.
58. Han,K., Jaimovich,A., Dey,G., Ruggero,D., Meyuhas,O., Sonenberg,N. and Meyer,T. (2013) Parallel measurement of dynamic changes in translation rates in single cells. *Nat. Methods*, **11**, 86–93.
59. Yoon,O.K. and Brem,R.B. (2010) Noncanonical transcript forms in yeast and their regulation during environmental stress. *RNA*, **16**, 1256–1267.
60. Waern,K. and Snyder,M. (2013) Extensive transcript diversity and novel upstream open reading frame regulation in yeast. *G3: Genes | Genomes | Genetics*, **3**, 343–352.
61. Waks,Z., Klein,A.M. and Silver,P.A. (2011) Cell-to-cell variability of alternative RNA splicing. *Mol. Syst. Biol.*, **7**, 506.
62. Hossain,M.A., Rodriguez,C.M. and Johnson,T.L. (2011) Key features of the two-intron Saccharomyces cerevisiae gene SUS1 contribute to its alternative splicing. *Nucleic Acids Res.*, **39**, 8612–8627.
63. Shalek,A.K., Satija,R., Adiconis,X., Gertner,R.S., Gaublomme,J.T., Raychowdhury,R., Schwartz,S., Yosef,N., Malboeuf,C., Lu,D. *et al.* (2013) Single-cell transcriptomics reveals bimodality in expression and splicing in immune cells. *Nature*, **498**, 236–240.
64. Iyer,S., Park,B.R. and Kim,M. (2016) Absolute quantitative measurement of transcriptional kinetic parameters in vivo. *Nucleic Acids Res.*, **44**, e142.
65. Kramer,S. (2016) Simultaneous detection of mRNA transcription and decay intermediates by dual colour single mRNA FISH on subcellular resolution. *Nucleic Acids Res.*, **45**, e49.
66. Wang,P.L., Bao,Y., Yee,M.-C., Barrett,S.P., Hogan,G.J., Olsen,M.N., Dinneny,J.R., Brown,P.O. and Salzman,J. (2014) Circular RNA is expressed across the eukaryotic tree of life. *PLoS One*, **9**, e90859.